

## A lead(II) toluene complex

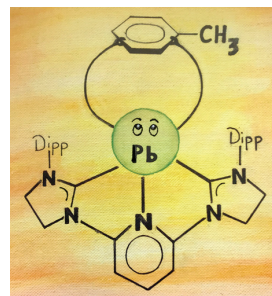
Julian Messelberger,<sup>a</sup> Piermaria Pinter,<sup>a,b</sup> Frank W. Heinemann<sup>b</sup> and Dominik Munz<sup>\*a</sup>

<sup>a</sup> *Inorganic Chemistry: Coordination Chemistry, Saarland University Campus, 66123 Saarbrücken, Germany.  
E-mail: dominik.munz@uni-saarland.de*

<sup>b</sup> *Department of Chemistry and Pharmacy, General and Inorganic Chemistry, Friedrich-Alexander-Universität Erlangen-Nürnberg (FAU), 91058 Erlangen, Germany*

DOI: 10.1016/j.mencom.2021.07.011

A well-defined intermolecular toluene complex of lead(II) supported by a pincer-type saNHC (saturated *N*-heterocyclic carbene) ligand was prepared through deprotonation of the bis(imidazolium) salt with  $\text{Pb}[\text{N}(\text{SiMe}_3)_2]_2$  or metalation of the free carbene and subsequent salt metathesis with  $\text{Tl}(\text{OTf})$ , followed by crystallization from toluene. Combined computational and experimental results indicate that noncovalent interactions with the lead atom ( $\sigma$ -hole type interaction, dispersion) and the diisopropylphenyl side groups of the ligand (dispersion) stabilize the complex.



**Keywords:** carbene complexes, pincer complexes, lead complexes, arene complexes, dispersion, non-covalent interaction, sigma-hole, energy decomposition analysis, electronic structure, DFT.

Arene complexes of transition metals, such as di(benzene)chromium,<sup>1</sup> are textbook examples in organometallic chemistry. The bonding between arenes and transition metals is described by the Dewar–Chatt–Duncanson (DCD) model (see Online Supplementary Materials, Figure S1, structure **S1**).<sup>2</sup> Inspired by the transition metal-like behavior of some *p*-block compounds, there is increasing interest in the chemistry of the main group elements.<sup>3</sup> This is particularly true for the heavy *p*-block elements, which, in analogy to the transition metals, switch redox states readily and are hence in principle suitable for redox-catalysis.<sup>4</sup> Also, arene complexes of the heavy *p*-block elements are known, although examples remain scarce.<sup>5</sup> In lack of *d*-orbitals of appropriate energy, the DCD concept is not applicable for the *p*-block elements.<sup>6</sup> Thus, ‘Menshutkin-type complexes’ (see Online Supplementary Materials, Figure S1, structure **S2**) may arguably be understood through the interaction of an arene donor orbital with a vacant acceptor orbital of the metal.<sup>7</sup> However, ‘non-covalent interactions’ (NCIs), *i.e.* electrostatic-,  $\pi$ - $\pi$ , dispersive or hydrophobic effects may be in many cases equally important. NCIs have been invoked in bio-<sup>8,9</sup> and supramolecular chemistry,<sup>10</sup> but have recently also found widespread attention in organic<sup>11</sup> and inorganic chemistry.<sup>12</sup> It has been recognized that steric bulk, associated with comparably strong dispersive interactions, is an excellent strategy to stabilize otherwise transient compounds such as, for instance, multiple bonded heavy *p*-block compounds.<sup>13</sup> Thus, for the bonding in arene complexes of *p*-block metals, the attractive interaction between  $\sigma$ -holes in the *p*-block element with the aromatic system of the arene has been invoked (see Online Supplementary Materials, Figure S1, structure **S3**).<sup>14</sup> This interaction is mostly electrostatic in nature. Others emphasized instead the importance of dispersion, which should be increasingly important for the heavy metals. However, additional computational studies on different  $\text{BiR}_3 \cdots \text{C}_6\text{H}_6$  compounds ( $\text{R} = \text{Me}, \text{OMe}, \text{Cl}$ ) outlined that the influence of substituents of the metal on the strength of

the dispersive interactions is more significant than the metal itself. For instance, the interaction in  $\text{Me}_3\text{Bi} \cdots \text{C}_6\text{H}_6$  is purely dispersive, whereas in  $\text{Cl}_3\text{Bi} \cdots \text{C}_6\text{H}_6$  also donor–acceptor interactions, exerted from charge transfer from benzene  $\pi$  orbitals into  $\text{BiCl}_3$   $\sigma^*$  orbitals, are almost equally important.<sup>15</sup> Experimental studies on intermolecular arene coordination compounds were dedicated to a handful of tin(II)<sup>16</sup> and thallium(I)<sup>17</sup> complexes.

Polymeric lead(II) **1** with coordinated benzene has been reported by Amma *et al.* in 1974 (Figure 1). Yet, examples of well-defined, electron-rich, monomeric  $\eta^6$   $\text{Pb}^{\text{II}}$  complexes with intermolecular arene interactions remain scarce. Rare examples with structural proof comprise compound **2** which coordinates toluene in an  $\eta^2$  fashion, as well as complex **3**.<sup>18</sup> Also examples for arene bonding of bismuth(III) have been described<sup>19</sup> and the stabilization due to toluene coordination was predicted to be 22  $\text{kJ mol}^{-1}$ .<sup>20</sup> Thereby, the ‘bond’ was rationalized by an orbital ‘ $\sigma + 2\pi^{5(d)}$ ’ interaction. Similar studies with electron-rich, monomeric lead compounds have not been reported to the best of our knowledge.

Herein, we present the synthesis of a toluene complex of lead(II), which is embedded in a CNC pincer-type saNHC (saturated *N*-heterocyclic carbene) ligand. The computational analysis suggests that the bonding interaction should be weak and mostly due to dispersive interactions with the metal as well

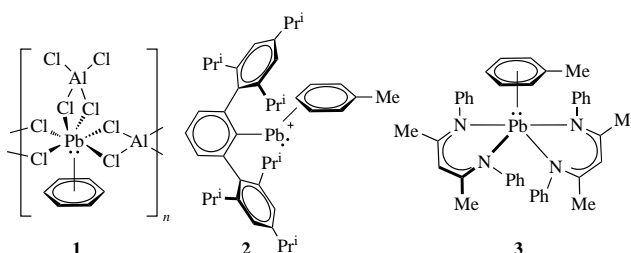
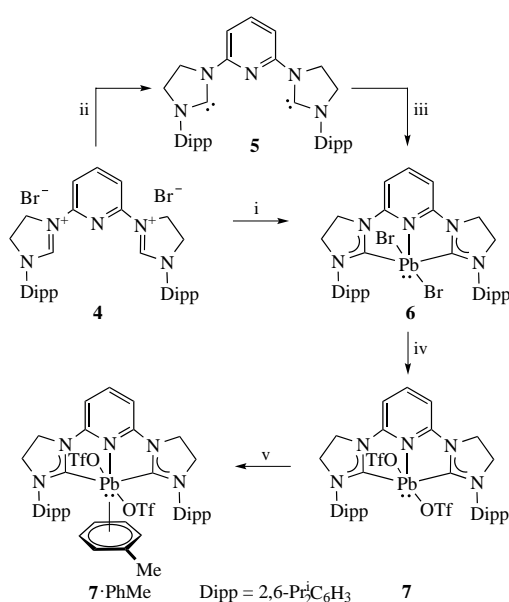


**Figure 1** Known arene lead complexes.

as to some extent the bulky arene substituents of the ligand. In the search for strongly polarized multiple bonds, namely vicinal zwitterions with low radicaloid character,<sup>21</sup> we started to investigate lead complexes. We were aiming at pyridine bridged NHC<sup>22</sup> complexes, which should provide favorable steric properties as well as stability. Note that pincer-type ligands have proven useful for the stabilization of reactive *p*-block complexes,<sup>23</sup> although NHC congeners have not yet received a lot of attention.<sup>24</sup> Treatment of known<sup>25</sup> imidazolium salt **4** with  $\text{Pb}[\text{N}(\text{SiMe}_3)_2]_2$  cleanly afforded the lead(II) complex **6** in quantitative yield (Scheme 1). Equally, generation of the free biscarbene through deprotonation with two equivalents of  $\text{KN}(\text{SiMe}_3)_2$  in the presence of  $\text{PbBr}_2$  gave, after workup, the same complex **6** in 76% yield, respectively. Compound **6** represents, to the best of our knowledge, the first example of a  $\pi$ -acidic saNHC coordinated lead complex. In its  $^1\text{H}$  NMR spectrum, two sets of signals are discernible for the eight protons of the backbone of the saNHC at 4.32 and 4.09 ppm, and the triplet for the proton in *para*-position of the pyridine moiety appears at 8.17 ppm. Further, the diisopropylphenyl (Dipp)–CH signal shows up as a septet at 3.14 ppm. The  $^1\text{H}$  NMR spectroscopic analysis indicates the formation of a  $C_{2v}$ -symmetric complex at the time scale of the NMR experiment. Interestingly, the  $^{13}\text{C}$  signal at 246.2 ppm, which was assigned to the imidazolidin-2-ylidene carbene carbon atoms, shifts slightly more downfield than in the free carbene **5** (243.8 ppm). In the  $^{207}\text{Pb}$  NMR spectrum, a signal at 187 ppm was observed.

Salt metathesis of compound **6** with two equivalents of TlOTf quantitatively gave **7** according to the NMR spectroscopic analysis. All  $^1\text{H}$  NMR signals (except for the aliphatic Dipp-signals) are shifted downfield in respect to **6**. Most prominently, the  $^{13}\text{C}$  NMR spectrum showed a significant downfield shift of the carbene signals to 252.4 ppm. Additionally, a new signal was observed in the  $^{19}\text{F}$  NMR at  $-77.7$  ppm. The signal in the  $^{207}\text{Pb}$  NMR shifted from 187 ppm in **6** to  $-430$  ppm, which we assign to the lead triflate compound **7**. To the best of our knowledge, no other (pseudo)octahedral NHC-supported lead(II) compounds are known. The  $^{207}\text{Pb}$  NMR signal of **7** is shifted downfield in comparison to reported three-coordinate (anionic) NHC/MIC complexes (1619, 1675 and 2841 ppm, respectively).<sup>26</sup> The same applies to three-coordinated ferrocene derived



**Scheme 1** Reagents and conditions: i,  $\text{Pb}[\text{N}(\text{SiMe}_3)_2]_2$ , THF,  $-78 \rightarrow 20$  °C, 16 h; ii,  $\text{KN}(\text{SiMe}_3)_2$  (2 equiv.), toluene,  $-40 \rightarrow 20$  °C, 30 min; iii,  $\text{PbBr}_2$ , THF, room temperature, 16 h; iv, TlOTf (2 equiv.), THF, room temperature, 16 h; v, PhMe, crystallization.

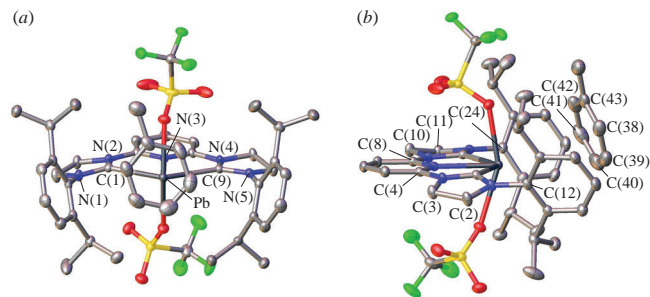


**Figure 2** Solid-state structure of complex **7-PhMe** shown (a) from the front and (b) from the side. Ellipsoids are shown at the 50% probability level; co-crystallized hexane and hydrogen atoms are omitted for clarity. For selected bond lengths and angles, see Online Supplementary Materials.

plumbylene–NHC complexes (2403 ppm,<sup>27</sup> 1395 ppm<sup>28</sup>). Only an NHC coordinate plumbocene was reported to shift more downfield with  $-4344$  ppm.<sup>29</sup> Subsequently, colourless needles, suitable for single crystal X-ray diffraction analysis, were obtained through condensing hexanes into a saturated solution in toluene.

The solid-state structure<sup>†</sup> of complex **7-PhMe** reveals that the lead atom shows a pseudo-octahedral coordination geometry with a Pb–N(pyridine) bond distance of 2.5416(18) Å, which is slightly elongated in comparison to the previously reported lead(II) pyridine complexes [2.466(6) Å].<sup>30</sup> The ligands are not distributed equally, *i.e.* the lead(II) is coordinated in a hemidirected<sup>31</sup> fashion with Pb–C(1) and Pb–C(2) bond lengths of 2.554(2) and 2.570(2) Å. The Pb–C(carbene) bonds are elongated in comparison to the previously reported ‘conventional NHC’ lead compounds, where the average bond length amounts to 2.517 Å (see Online Supplementary Materials, Table S3). Lead complexes with the only marginally  $\pi$ -acidic mesoionic carbene (MIC) ligands show bond lengths of 2.367(9), 2.351(10), 2.393(9) and 2.397(10) Å.<sup>26</sup> For the only other lead complex with a significantly  $\pi$ -acidic carbene ligand, namely a benzimidazolin-2-ylidene (benzNHC), a comparable bond length of 2.586(7) Å was found.<sup>32</sup>

Further, we note that the nitrogen atoms of the saNHC are devoid of pyramidalization [ $\Sigma_{\text{N}(1)}$ : 359.99°;  $\Sigma_{\text{N}(2)}$ : 359.68°;  $\Sigma_{\text{N}(4)}$ : 359.32°;  $\Sigma_{\text{N}(5)}$ : 359.26°;  $\Sigma = 360^\circ$  for a perfectly planar  $\text{NR}_3$  group] resulting in an unusual planar imidazolidine ring ( $\Sigma_{-\text{C}(2)-\text{N}(1)-\text{C}(1)-\text{N}(2)-\text{C}(3)-}$ : 539.74°;  $\Sigma_{-\text{C}(10)-\text{N}(4)-\text{C}(9)-\text{N}(5)-\text{C}(11)-}$ : 537.08°;  $\Sigma = 540^\circ$  for a perfectly planar imidazolidine ring). This indicates enhanced  $\pi$ -donation from the amines’ lone pairs into the formally vacant carbene  $\pi$ -orbital. The Pb–C bonds to the toluene molecule vary significantly with bond distances ranging from 3.728 to 4.398 Å (average: 4.070 Å), which is longer than the reported Pb–toluene bonds in **2** (3.616 Å).<sup>18(a)</sup>

<sup>†</sup> Crystal data for **7-PhMe**.  $\text{C}_{37}\text{H}_{45}\text{F}_6\text{N}_5\text{O}_6\text{PbS}_2 \cdot \text{C}_7\text{H}_8 \cdot 0.5 \text{C}_6\text{H}_{14}$  ( $M = 1176.31$ ), monoclinic, space group  $P2_1/c$  at 100 K:  $a = 20.6674(12)$ ,  $b = 13.1044(7)$  and  $c = 18.8317(10)$  Å,  $\beta = 98.208(2)^\circ$ ,  $V = 5050.5(5)$  Å<sup>3</sup>,  $Z = 4$ ,  $d_{\text{calc}} = 1.547$  g cm<sup>-3</sup>,  $\mu(\text{MoK}\alpha) = 3.50$  mm<sup>-1</sup>,  $F(000) = 2372$ . Total of 224327 reflections were collected (15425 independent reflections,  $R_{\text{int}} = 0.056$ ) and used in the refinement, which converged to  $wR_2$  0.0509, GOOF 1.062 for all independent reflections [ $R_1 = 0.0241$  was calculated for 15425 reflections with  $I \geq 2\sigma(I)$ ]. The X-ray diffraction analysis was carried out on a Bruker Kappa Photon 2  $\mu\text{mS}$  Duo diffractometer (MoK $\alpha$  radiation,  $\lambda = 0.71073$  Å, graphite monochromator). Data were corrected for Lorentz and polarization effects; semiempirical absorption corrections were performed on the basis of multiple scans using SADABS.<sup>33</sup> The structure was solved by direct methods (SHELXT)<sup>34</sup> and refined by full-matrix least-squares procedures on  $F^2$  using SHELXL 2018/3.<sup>35</sup> OLEX2 was used to prepare material for publication.<sup>36</sup>

CCDC 2074842 contains the supplementary crystallographic data for this paper. These data can be obtained free of charge from The Cambridge Crystallographic Data Centre via <http://www.ccdc.cam.ac.uk>.

To elucidate the nature of the lead–toluene interaction, quantum chemical calculations were performed. Among various functionals (BP86,<sup>37</sup> B3LYP,<sup>38</sup> PBE0<sup>39</sup>) investigated, PBE0 gave the best fit (Table S4) with the geometric parameters obtained from the XRD analysis. Using the PBE0-D3/ZORA-def2-TZVPP//PBE0-D3/ZORA-def2-SVP level of theory (lead: SARC-def2-TZVPP), the reaction of **7** and toluene was predicted to be slightly exergonic ( $\Delta E = -68 \text{ kJ mol}^{-1}$ ,  $\Delta G = -7 \text{ kJ mol}^{-1}$ ) in the gas-phase, yet isoergic in benzene or toluene solutions (CPCM;  $\Delta E = -64 \text{ kJ mol}^{-1}$ ,  $\Delta G = 0 \text{ kJ mol}^{-1}$ ) assuming 1 M concentration of both reactants. Also, in more polar solutions, such as chloroform, the formation of complex **7**·PhMe was predicted to be isoergic (CPCM;  $\Delta E = -63 \text{ kJ mol}^{-1}$ ,  $\Delta G = 0 \text{ kJ mol}^{-1}$ ). Indeed, the <sup>1</sup>H NMR spectroscopic analysis (Figure S9) indicated the dissociation of toluene upon dissolution of crystals of **7**·PhMe in CDCl<sub>3</sub>.

To further understand the nature of the weak interaction with the toluene molecule, NOCV-EDA<sup>40</sup> (Natural Orbitals for Chemical Valence – Energy Decomposition Analysis) at the PBE0-D3/ZORA-def2-TZVPP//PBE0-D3/ZORA-def2-SVP (lead: SARC-ZORA-TZVPP//SARC-ZORA-TZVP) level of theory was performed.<sup>15(b)</sup> The attractive interactions are governed by dispersive interactions ( $-58 \text{ kJ mol}^{-1}$ ), but also the combined Pauli repulsive and electrostatic term is attractive ( $-39 \text{ kJ mol}^{-1}$ ). Contrarily, the orbital interaction is repulsive by  $+27 \text{ kJ mol}^{-1}$ , whereas the preparation energy penalty ( $+2 \text{ kJ mol}^{-1}$ ) contributes only marginally to the overall reaction energy (Table S1). Additionally, *ab-initio* LED<sup>41</sup> (Local Energy Decomposition) analysis using the Domain-based Local Pair Natural Orbitals Coupled Cluster (DLPNO-CCSD(T)/def2-TZVPP) level of theory was performed. The formation of the lead(II) toluene complex is predicted to be exoergic in the gas phase by  $-73 \text{ kJ mol}^{-1}$ . In addition to the geometric preparation energy  $\Delta E_{\text{geo,prep}}$  of  $+5 \text{ kJ mol}^{-1}$ , the LED analysis suggests a repulsive HF interaction of  $+44 \text{ kJ mol}^{-1}$ , whereas the dispersive interactions are calculated to be impressive  $-98 \text{ kJ mol}^{-1}$ . Non-dispersive contributions as well as the triples correction account as well for considerable attractive interactions ( $-24 \text{ kJ mol}^{-1}$ , Table S2).

To visualize the attractive and repulsive interactions in complex **7**·PhMe, we applied Yang's non-covalent interaction (NCI) method.<sup>42</sup> The isosurface of the NCI plot is dependent on both the electron density and its first derivative (Figure 3).<sup>43</sup> This reduced density gradient is a dimensionless quantity that can be used to describe the deviation from a homogeneous electron distribution.<sup>44</sup> Consequently, this value will be very low in regions of covalent and non-covalent interactions. The isosurface can be plotted and the different types of interactions (*i.e.* changes in the reduced density gradient) can be visualized using different colors. Thereby, blue indicates an attractive interaction, whereas green implies weak interactions, such as Van der Waals forces. Conversely, brown or red coloring reveals medium to strong repulsion [see Figure 3(a),(b)]. The plot corroborates attractive interaction with the metal as well as with the Dipp substituents. Also, the scatter plot indicates weak interactions (Figure S11). Examining the electrostatic potential map of toluene-free complex **7** showed significant positive polarization around the lone pair of the central lead atom. This  $\sigma$ -hole-type interaction with the  $\pi$ -electrons of the toluene ligand (Figure S12, blue) accounts to some extent for the stability of the arene complex **7**·PhMe. To unambiguously clarify the importance of the Dipp groups, calculations where the Dipp groups were truncated by hydrogen atoms were performed. Intriguingly, the D3 correction suggests for the latter compound overall only  $-25 \text{ kJ mol}^{-1}$  stabilization through dispersive effects. This is  $+33 \text{ kJ mol}^{-1}$  less than obtained for **7**·PhMe ( $-58 \text{ kJ mol}^{-1}$ ; *vide supra*). This confirms that both and the lead atom with its lone pair the

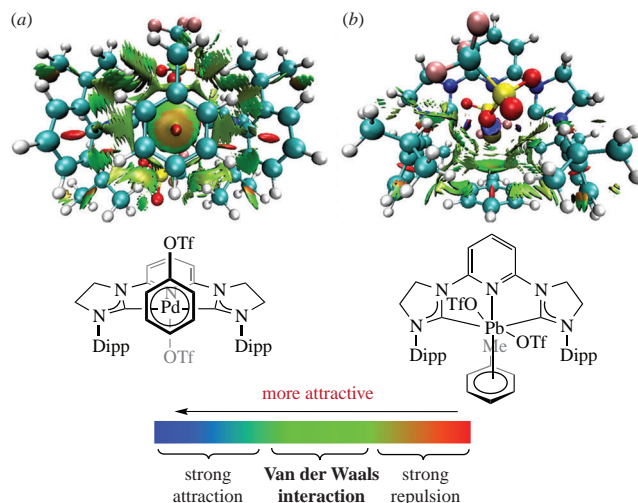


**Figure 3** NCI isosurface (isoval: 0.5) for **7**·PhMe, which is depicted from the bottom (a) and front (b) to illustrate the interaction between lead and toluene.

flanking Dipp groups contribute significantly to the overall attractive interaction in **7**·PhMe.

In conclusion, we have described the preparation and spectroscopic analysis of an intermolecular lead(II) toluene complex with a pincer-type saNHC ligand with ancillary diisopropylphenyl substituents. According to computational studies (non-covalent interaction NCI method, energy decomposition analysis), the attractive interactions are largely due to weak interactions with both the lead atom ( $\sigma$ -hole-type, dispersion) as well as the two flanking diisopropylphenyl groups (dispersion). This finding will be useful for investigations in self-assembly, sensing, and supramolecular chemistry with heavy metals.

D. M. thanks the Fonds der Chemischen Industrie im Verband der Chemischen Industrie for a Liebig fellowship as well as the German-American Fulbright Commission for financial support through a Fulbright-Cotrell Award. We thank the RRZ Erlangen for computational resources.

#### Online Supplementary Materials

Supplementary data associated with this article can be found in the online version at doi: 10.1016/j.mencom.2021.07.011.

#### References

- E. O. Fischer and W. Hafner, *Z. Naturforsch. B: J. Chem. Sci.*, 1955, **10**, 665.
- (a) M. J. S. Dewar, *Bull. Soc. Chim. Fr.*, 1951, **18**, C71; (b) J. Chatt, L. A. Duncanson and L. M. Venanzi, *J. Chem. Soc.*, 1955, 4456; (c) J. Chatt and L. A. Duncanson, *J. Chem. Soc.*, 1953, 2939.
- P. P. Power, *Nature*, 2010, **463**, 171.
- F. Hanus, L. Groll and S. Inoue, *Chem. Sci.*, 2021, **12**, 2001.
- (a) H. Lüth and E. L. Amma, *J. Am. Chem. Soc.*, 1969, **91**, 7515; (b) M. S. Weininger, P. F. Rodesiler, A. G. Gash and E. L. Amma, *J. Am. Chem. Soc.*, 1972, **94**, 2135; (c) P. F. Rodesiler, E. L. Amma and T. Auel, *J. Am. Chem. Soc.*, 1975, **97**, 7405; (d) H. Schmidbaur, *Angew. Chem., Int. Ed.*, 1985, **24**, 893; (e) A. Schier, J. M. Wallis, G. Müller and H. Schmidbaur, *Angew. Chem., Int. Ed.*, 1986, **25**, 757; (f) W. Frank, J. Weber and E. Fuchs, *Angew. Chem., Int. Ed.*, 1987, **26**, 74; (g) T. Probst, O. Steigelmann, J. Riede and H. Schmidbaur, *Angew. Chem., Int. Ed.*, 1990, **29**, 1397; (h) H. Schmidbaur and A. Schier, *Organometallics*, 2008, **27**, 2361.
- J. Grunenberg, *Int. J. Quantum Chem.*, 2017, **117**, e25359.
- M. M. Watt, M. S. Collins and D. W. Johnson, *Acc. Chem. Res.*, 2013, **46**, 955.
- (a) V. L. Malinovskii, F. Samain and R. Häner, *Angew. Chem.*, 2007, **119**, 4548; (b) R. Fasan, R. L. A. Dias, K. Moehle, O. Zerbe, D. Obrecht, P. R. E. Mittl, M. G. Grütter and J. A. Robinson, *ChemBioChem*, 2006, **7**, 515.

- 9 (a) E. A. Meyer, R. K. Castellano and F. Diederich, *Angew. Chem., Int. Ed.*, 2003, **42**, 1210; (b) H. T. Chifotides and K. R. Dunbar, *Acc. Chem. Res.*, 2013, **46**, 894.
- 10 (a) I. Caracelli, I. Haiduc, J. Zukerman-Schpector and E. R. T. Tiekink, *Coord. Chem. Rev.*, 2014, **281**, 50; (b) M. A. Pitt and D. W. Johnson, *Chem. Soc. Rev.*, 2007, **36**, 1441; (c) I. Caracelli, I. Haiduc, J. Zukerman-Schpector and E. R. T. Tiekink, *Coord. Chem. Rev.*, 2013, **257**, 2863; (d) I. Caracelli, J. Zukerman-Schpector, I. Haiduc and E. R. T. Tiekink, *CrystEngComm*, 2016, **18**, 6960; (e) E. R. T. Tiekink and J. Zukerman-Schpector, *Aust. J. Chem.*, 2010, **63**, 535; (f) V. M. Cangelosi, M. A. Pitt, W. J. Vickaryous, C. A. Allen, L. N. Zakharov and D. W. Johnson, *Cryst. Growth Des.*, 2010, **10**, 3531; (g) E. R. T. Tiekink and J. Zukerman-Schpector, *The Importance of Pi-Interactions in Crystal Engineering: Frontiers in Crystal Engineering*, John Wiley & Sons, Ltd., Chichester, 2012; (h) D.-X. Wang and M.-X. Wang, *J. Am. Chem. Soc.*, 2013, **135**, 892; (i) O. Perraud, V. Robert, H. Gornitzka, A. Martinez and J. P. Dutasta, *Angew. Chem., Int. Ed.*, 2012, **51**, 504.
- 11 (a) P. R. Schreiner, L. V. Chernish, P. A. Gunchenko, E. Yu. Tikhonchuk, H. Hausmann, M. Serafin, S. Schlecht, J. E. P. Dahl, R. M. K. Carlson and A. A. Fokin, *Nature*, 2011, **477**, 308; (b) A. A. Fokin, L. V. Chernish, P. A. Gunchenko, E. Y. Tikhonchuk, H. Hausmann, M. Serafin, J. E. P. Dahl, R. M. K. Carlson and P. R. Schreiner, *J. Am. Chem. Soc.*, 2012, **134**, 13641; (c) M. Stein, W. Winter and A. Rieker, *Angew. Chem., Int. Ed.*, 1978, **17**, 692.
- 12 (a) D. J. Liprot and P. P. Power, *Nat. Rev. Chem.*, 2017, **1**, 0004; (b) C. L. Wagner, L. Tao, E. J. Thompson, T. A. Stich, J. Guo, J. C. Fettinger, L. A. Berben, R. D. Britt, S. Nagase and P. P. Power, *Angew. Chem., Int. Ed.*, 2016, **55**, 10444.
- 13 (a) P. P. Power, *Chem. Rev.*, 1999, **99**, 3463; (b) P. P. Power, *Organometallics*, 2020, **39**, 4127; (c) J. P. Wagner and P. R. Schreiner, *Angew. Chem., Int. Ed.*, 2015, **54**, 12274.
- 14 (a) R. Lo, P. Švec, Z. Růžičková, A. Růžička and P. Hobza, *Chem. Commun.*, 2016, **52**, 3500; (b) A. Bauzá, D. Quiñero, P. M. Deyà and A. Frontera, *Phys. Chem. Chem. Phys.*, 2012, **14**, 14061; (c) A. Bauzá, D. Quiñero, P. M. Deyà and A. Frontera, *CrystEngComm*, 2013, **15**, 3137; (d) T. Clark, M. Hennemann, J. S. Murray and P. Politzer, *J. Mol. Model.*, 2007, **13**, 291; (e) P. Politzer, J. S. Murray and T. Clark, *Phys. Chem. Chem. Phys.*, 2013, **15**, 11178.
- 15 (a) M. Krasowska, W. B. Schneider, M. Mehring and A. A. Auer, *Chem. – Eur. J.*, 2018, **24**, 10238; (b) A. A. Auer, D. Mansfeld, C. Nolde, W. Schneider, M. Schürmann and M. Mehring, *Organometallics*, 2009, **28**, 5405; (c) A.-M. Preda, M. Krasowska, L. Wrobel, P. Kitschke, P. C. Andrews, J. G. MacLellan, L. Mertens, M. Korb, T. Ruffer, H. Lang, A. A. Auer and M. Mehring, *Beilstein J. Org. Chem.*, 2018, **14**, 2125.
- 16 A. Schäfer, F. Winter, W. Saak, D. Haase, R. Pöttgen and T. Müller, *Chem. – Eur. J.*, 2011, **17**, 10979.
- 17 Y. Sarazin, D. L. Hughes, N. Kaltsoyannis, J. A. Wright and M. Bochmann, *J. Am. Chem. Soc.*, 2007, **129**, 881.
- 18 (a) E. C. Y. Tam, M. P. Coles, J. D. Smith and J. R. Fulton, *Polyhedron*, 2015, **85**, 284; (b) H. Schmidbauer, W. Bublak, B. Huber, J. Hofmann and G. Müller, *Chem. Ber.*, 1989, **122**, 265; (c) L. G. Ranis, K. Werellapatha, N. J. Pietrini, B. A. Bunker and S. N. Brown, *Inorg. Chem.*, 2014, **53**, 10203; (d) W. Frank and F.-G. Wittmer, *Chem. Ber.*, 1997, **130**, 1731; (e) A. G. Gash, P. F. Rodesiler and E. L. Amma, *Inorg. Chem.*, 1974, **13**, 2429; (f) S. Hino, M. Brynda, A. D. Phillips and P. P. Power, *Angew. Chem.*, 2004, **116**, 2709; (g) D. Labahn, F. M. Bohnen, R. Herbst-Irmer, E. Pohl, D. Stalke and H. W. Roesky, *Z. Anorg. Allg. Chem.*, 1994, **620**, 41; (h) D. J. Teff, J. C. Huffman and K. G. Caulton, *Inorg. Chem.*, 1997, **36**, 4372; (i) F. T. Edelmann, J.-K. F. Buijink, S. A. Brooker, R. Herbst-Irmer, U. Kilimann and F. M. Bohnen, *Inorg. Chem.*, 2000, **39**, 6134.
- 19 (a) J. Fanfrlík, R. Sedlak, A. Pecina, L. Rulíšek, L. Dostál, J. Moncól', A. Růžička and P. Hobza, *Dalton Trans.*, 2016, **45**, 462; (b) C. Silvestru, H. J. Breunig and H. Althaus, *Chem. Rev.*, 1999, **99**, 3277; (c) M. Krasowska, A.-M. Fritzsche, M. Mehring and A. A. Auer, *ChemPhysChem*, 2019, **20**, 2539; (d) C. Hering-Junghans, A. Schulz, M. Thomas and A. Villinger, *Dalton Trans.*, 2016, **45**, 6053.
- 20 L. E. Turner, M. G. Davidson, M. D. Jones, H. Ott, V. S. Schulz and P. J. Wilson, *Inorg. Chem.*, 2006, **45**, 6123.
- 21 (a) A. Grünwald, F. W. Heinemann and D. Munz, *Angew. Chem., Int. Ed.*, 2020, **59**, 21088; (b) D. Munz, *Chem. Sci.*, 2018, **9**, 1155; (c) A. Grünwald, N. Orth, A. Scheurer, F. W. Heinemann, A. Pöthig and D. Munz, *Angew. Chem., Int. Ed.*, 2018, **57**, 16228; (d) A. Grünwald and D. Munz, *J. Organomet. Chem.*, 2018, **864**, 26.
- 22 (a) M. N. Hopkinson, C. Richter, M. Schedler and F. Glorius, *Nature*, 2014, **510**, 485; (b) R. S. Ghadwal, *Dalton Trans.*, 2016, **45**, 16081; (c) D. Munz, *Organometallics*, 2018, **37**, 275; (d) A. J. Arduengo and G. Bertrand, *Chem. Rev.*, 2009, **109**, 3209; (e) *N-Heterocyclic Carbenes: From Laboratory Curiosities to Efficient Synthetic Tools*, ed. S. Díez-González, Royal Society of Chemistry, Cambridge, 2000; (f) T. Rovis and S. P. Nolan, *Synlett*, 2013, **24**, 1188; (g) *N-Heterocyclic Carbenes: Effective Tools for Organometallic Synthesis*, ed. S. P. Nolan, Wiley, 2014; (h) H. V. Huynh, *The Organometallic Chemistry of N-Heterocyclic Carbenes*, Wiley, 2017; (i) F. E. Hahn, *Chem. Rev.*, 2018, **118**, 9455; (j) M. Melaimi, M. Soleilhavou and G. Bertrand, *Angew. Chem., Int. Ed.*, 2010, **49**, 8810; (k) V. Nesterov, D. Reiter, P. Bag, P. Frisch, R. Holzner, A. Porzelt and S. Inoue, *Chem. Rev.*, 2018, **118**, 9678; (l) A. Röther and R. Kretschmer, *J. Organomet. Chem.*, 2020, **918**, 121289; (m) J. A. Mata, M. Poyatos and E. Peris, *Coord. Chem. Rev.*, 2007, **251**, 841; (n) A. Grünwald, S. J. Goodner and D. Munz, *J. Visualized Exp.*, 2019, e59389.
- 23 (a) O. Planas, F. Wang, M. Leutzsch and J. Cornella, *Science*, 2020, **367**, 313; (b) J. M. Lipshultz, G. Li and A. T. Radosevich, *J. Am. Chem. Soc.*, 2021, **143**, 1699; (c) S. Lim and A. T. Radosevich, *J. Am. Chem. Soc.*, 2020, **142**, 16188; (d) M. B. Kindervater, K. M. Marczenko, U. Werner-Zwanziger and S. S. Chitnis, *Angew. Chem., Int. Ed.*, 2019, **58**, 7850; (e) Y. Pang, M. Leutzsch, N. Nöthling and J. Cornella, *J. Am. Chem. Soc.*, 2020, **142**, 19473.
- 24 (a) L. Dostál, *Coord. Chem. Rev.*, 2017, **353**, 142; (b) A. Koch, S. Kriek, H. Görls and M. Westerhausen, *Organometallics*, 2017, **36**, 994; (c) A. Koch, S. Kriek, H. Görls and M. Westerhausen, *Organometallics*, 2017, **36**, 2811.
- 25 (a) R. P. Yu, D. Hesk, N. Rivera, I. Pelczer and P. J. Chirik, *Nature*, 2016, **529**, 195; (b) J. Messelberger, A. Grünwald, P. Stegner, L. Senft, F. W. Heinemann and D. Munz, *Inorganics*, 2019, **7**, 65.
- 26 J. B. Waters, L. S. Tucker and J. M. Goicoechea, *Organometallics*, 2018, **37**, 655.
- 27 R. Guthardt, J. Oetzel, J. I. Schweizer, C. Bruhn, R. Langer, M. Maurer, J. Vícha, P. Shestakova, M. C. Holthausen and U. Siemeling, *Angew. Chem., Int. Ed.*, 2019, **58**, 1387.
- 28 D. Kargin, Z. Kelemen, K. Krekić, L. Nyulászi and R. Pietschnig, *Chem. – Eur. J.*, 2018, **24**, 16774.
- 29 S. Danés, C. Müller, L. Wirtz, V. Huch, T. Block, R. Pöttgen, A. Schäfer and D. M. Andrada, *Organometallics*, 2020, **39**, 516.
- 30 D. L. Reger, T. D. Wright, M. D. Smith, A. L. Rheingold, S. Kassel, T. Concolino and B. Rhagitan, *Polyhedron*, 2002, **21**, 1795.
- 31 L. Shimoni-Livny, J. P. Glusker and C. W. Bock, *Inorg. Chem.*, 1998, **37**, 1853.
- 32 B. Gehrhuis, P. B. Hitchcock and M. F. Lappert, *Dalton Trans.*, 2000, 3094.
- 33 L. Krause, R. Herbst-Irmer, G. M. Sheldrick and D. Stalke, *J. Appl. Crystallogr.*, 2015, **48**, 3.
- 34 G. M. Sheldrick, *Acta Crystallogr.*, 2015, **A71**, 3.
- 35 G. M. Sheldrick, *Acta Crystallogr.*, 2015, **C71**, 3.
- 36 O. V. Dolomanov, L. J. Bourhis, R. J. Gildea, J. A. K. Howard and H. Puschmann, *J. Appl. Crystallogr.*, 2009, **42**, 339.
- 37 (a) A. D. Becke, *Phys. Rev. A*, 1988, **38**, 3098; (b) J. P. Perdew, *Phys. Rev. B*, 1986, **33**, 8822.
- 38 (a) A. D. Becke, *J. Chem. Phys.*, 1993, **98**, 5648; (b) C. T. Lee, W. T. Yang and R. G. Parr, *Phys. Rev. B*, 1988, **37**, 785.
- 39 (a) C. Adamo and V. Barone, *J. Chem. Phys.*, 1999, **110**, 6158; (b) J. P. Perdew, K. Burke and M. Ernzerhof, *Phys. Rev. Lett.*, 1996, **77**, 3865; (c) J. P. Perdew, M. Ernzerhof and K. Burke, *J. Chem. Phys.*, 1996, **105**, 9982.
- 40 (a) K. Morokuma, *J. Chem. Phys.*, 1971, **55**, 1236; (b) T. Ziegler and A. Rauk, *Inorg. Chem.*, 1979, **18**, 1755; (c) T. Ziegler and A. Rauk, *Inorg. Chem.*, 1979, **18**, 1558.
- 41 W. B. Schneider, G. Bistoni, M. Sparta, M. Saitow, C. Riplinger, A. A. Auer and F. Neese, *J. Chem. Theory Comput.*, 2016, **12**, 4778.
- 42 (a) E. R. Johnson, S. Keinan, P. Mori-Sánchez, J. Contreras-García, A. J. Cohen and W. Yang, *J. Am. Chem. Soc.*, 2010, **132**, 6498; (b) J. Contreras-García, E. R. Johnson, S. Keinan, R. Chaudret, J.-P. Piquemal, D. N. Beratan and W. Yang, *J. Chem. Theory Comput.*, 2011, **7**, 625.
- 43 T. Lu and F. Chen, *J. Comput. Chem.*, 2012, **33**, 580.
- 44 (a) P. Hohenberg and W. Kohn, *Phys. Rev. B*, 1964, **136**, 864; (b) A. D. Becke, in *Modern Electronic Structure Theory*, ed. D. R. Yarkony, World Scientific, River Edge, NJ, 1995, pp. 1022–1047; (c) A. J. Cohen, P. Mori-Sánchez and W. Yang, *Science*, 2008, **321**, 792.

Received: 1st April 2021; Com. 21/6512